

GHGT-10

Studies on Corrosion and Corrosion Inhibitors for Amine Based Solvents for CO₂ Absorption from Power Plant Flue Gases Containing CO₂, O₂ and SO₂

Nattawan Kladkaew^a, Raphael Idem^{b1*}, Paitoon Tontiwachwuthikul^b, Chintana Saiwan^a

^a*Petrochemical and Petroleum College, Chulalongkorn University, Pathumwan, Bangkok, Thailand, 10330*

^b*Process Systems Engineering, Faculty of Engineering, University of Regina, Regina, Saskatchewan, Canada S4S 0A2*

Abstract

This work investigated the effects of operating parameters on the corrosion of carbon steel in MEA-H₂O-CO₂-O₂-SO₂ systems. It also investigated the effectiveness of a number of chemical additives in inhibiting corrosion. Two methods, namely, the Tafel plot and potentiodynamic polarization techniques were used to quantify the corrosion rate. The results showed that an increase of both O₂ and SO₂ concentrations in simulated flue gas stream, CO₂ loading, MEA concentration and the operating temperature induced higher corrosion rates. Also, the data obtained from different corrosion measurement techniques produced almost the same results. In addition, the corrosion products obtained experimentally based on CE and SEM/EDS measurements included Fe(OH)₂, Fe(OH)₃, 2Fe₂O₃·H₂O, FeCO₃, and FeSO₄. A power-law model shows that CO₂ loading had the highest impact on the corrosion rate, while SO₂ and O₂ show only slight effects on the corrosion rate. It was observed that all of the corrosion inhibitors tested can minimize corrosion of carbon steel in the MEA-H₂O-CO₂-O₂-SO₂ system. However, the inhibition efficiency of each inhibitor depended on its concentration.

© 2011 Published by Elsevier Ltd. Open access under [CC BY-NC-ND license](http://creativecommons.org/licenses/by-nc-nd/3.0/).

Keywords: Corrosion, Inhibitor, CO₂ capture, Monoethanolamine, SO₂

1. Introduction

Power plant flue gases are a major source of carbon dioxide (CO₂) emissions. A control technique must be in place to mitigate CO₂ in order to prevent its enhanced greenhouse effect. Chemical absorption with aqueous amine solutions has been found to be an effective CO₂ capture especially for low-pressure flue gas streams. However, depending on the operating conditions, there could be a major drawback associated with corrosion in certain sections of the CO₂ plant resulting in reduced efficiency and increased operating cost of the process. Operating parameters including the process temperature, amine concentration, dissolved CO₂ and some degradation products have been reported to induce corrosion in amine units [1, 2]. As well, the composition of flue gas especially the presence of sulfur dioxide (SO₂) known as a corrosive species can potentially give rise to plant equipment damage.

* Corresponding author. Tel.: 01-306-585-4470; fax: 01-306-585-4855.

E-mail address: Raphael.idem@uregina.ca.

So far, the effect of SO₂ in flue gas stream on corrosion in the CO₂ capture process has not been reported. Then, two popular corrosion measurement techniques, Tafel plot and potentiodynamic, are used in this work in order to quantify the obtained corrosion rate. Also, in order to understand how corrosion products are produced, some corrosion mechanisms or pathways have been postulated. Moreover, this work also focused on investigating corrosion minimization by using various corrosion inhibitors. Various chemical additives, namely, inhibitors A, B, C, D, E, and their blends were screened and tested for inhibition efficiency in MEA-H₂O-CO₂-O₂-SO₂ system. Corrosion inhibitor experiments were conducted by using a 273A potentiostat unit operating under severe corrosive conditions.

2. Experimental Section

2.1 Equipment and Chemicals

The electrochemical experiments were carried out using monoethanolamine (Fisher Scientific, ON) as the absorption solvent. It was diluted with deionized water to the desired concentration, which was accurately determined by titration with 1.0 N hydrochloric acid (HCl) solution using methyl orange as the titration indicator. The desired concentration of aqueous MEA solution was then preloaded with carbon dioxide to obtain the desired CO₂ loading (mol CO₂/mol MEA) by purging a stream of CO₂ gas (Praxair, research grade, ON) into the solution. The CO₂ loading procedure followed the Association of Official Analytical Chemists (AOAC) method [3]. The desired CO₂ loading was determined by titrating with the 1.0 N HCl solution using a Chittick apparatus. Electrochemical techniques were used to study corrosion of carbon steel C1020 (Metal Samples Company, AL) in an MEA-H₂O-CO₂-O₂-SO₂ system. The experiment setup consisted of an ASTM corrosion cell, potentiostat, water bath with temperature controller, condenser, gas supply set, and data acquisition system. An ASTM corrosion cell model K47 (London Scientific, Ltd., ON) was a 1 L flat bottom flask with ground glass joints. It is composed of one working electrode mounted with specimen; two high density carbon graphite rods used as counter electrodes, one reference electrode which is a mercurous sulfate electrode (MSE), one bridge tube, and a glass inlet and outlet for transferring gas to and from the corrosion cell. A potentiostat model 273A (London Scientific, Ltd., ON) was used to control the potential and to read the current accurately. PowerCORR version 2.47 (London Scientific, Ltd., ON) was used to acquire and analyze the experimental data. A water bath with a temperature controller was used to control the operating temperature. A condenser was connected to the corrosion cell to maintain the temperature in order to maintain the solution concentration in the cell by preventing evaporation during the experiment. The gas supply sets were gaseous mixtures of SO₂-O₂-N₂ that were similar to actual flue gas stream conditions.

2.2 Typical Experiment Run

The corrosion cell containing about 1 L of the tested solution which varied either the MEA concentration or the CO₂ loading, was immersed in a water bath with a temperature controller. The temperature of the solution was kept constant at the tested temperature. The desired simulated flue gas of O₂-SO₂/N₂ mixture was introduced into the corrosion cell at a flow rate of 150 mL/min for 1.5 h. The carbon rods counter electrodes were placed in the test cell. Then, the salt bridge was filled with the test solution and placed in the corrosion cell. The prepared surface was mounted on the electrode holder rod. The specimen was degreased with methanol and rinsed in distilled water just prior to immersion in the test cell. The salt-bridge probe tip was adjusted close to the specimen electrode. All the lines between the corrosion cell and the model 273A potentiostat had been connected before the corrosion potential (E_{CORR}) versus the MSE reference electrode of the test system were measured for at least 1 h to ensure that the corrosion potential value remained constant. Finally, the electrochemical experiment was started by using two different corrosion measurement techniques, which are Tafel plot and potentiodynamic polarization technique. Details of the corrosion measurement technique followed our previous work [4]. The information of the analysis of corrosion products by using Capillary Electrophoresis (CE) and Scanning Electron Microscopy-Energy Dispersive Spectrometry (SEM-EDS) followed our previous work as well [5].

2.3 Corrosion inhibitor

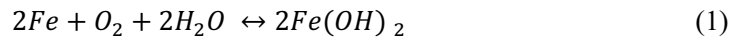
Five corrosion inhibitors were investigated for their inhibition effectiveness. These were: organic chemicals (A, B and D), inorganic chemical (C) and a commercial inhibitor (E). Inhibitor E has been used in one of the CO₂ capture pilot plants of the International Test Centre for CO₂ Capture (ITC) at the University of Regina. The combination of inhibitors was chosen based on the initial proposal of inhibiting behavior. Synergistic effects of blended inhibitors were investigated using their optimum concentrations. A known concentration of the inhibitor was introduced into the corrosion cell containing 1 L of 7 kmol/m³ MEA, CO₂ loading of 0.5 mol CO₂/mol MEA solution and the test procedure followed was the same as the one described by using 6% O₂, 204 ppm SO₂ at 353 K, which was chosen to represent a severe corrosive.

3. Results and Discussion

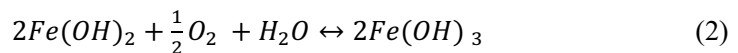
3.1 Effect of Operating Parameters

3.1.1 Oxygen Concentration

The corrosion rate increases as oxygen concentration increases. This is because the higher the oxygen concentrations, the higher the dissolved oxygen present in the tested solution resulting in the dissolution of iron. The reduction-oxidation reaction among iron, dissolved oxygen, and water occurs as in reaction 1 [6].



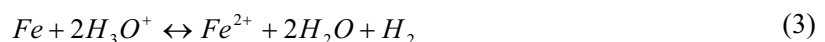
The produced ferrous hydroxide component (Fe(OH)₂) is unstable in systems containing oxygen and thus is oxidized to the ferric salt (Fe(OH)₃) or rust [6] as



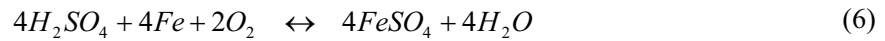
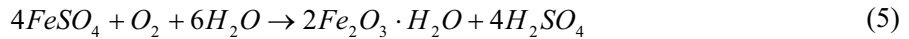
Only carbonate and bicarbonate inorganic anions were detected together by the CE technique in the tested solution. There is no significant change in the amount of carbonate/bicarbonate anions in the tested solution for different oxygen concentrations. This is because each of the tested solutions contained the same amount of dissolved carbon dioxide. It is well-known that the carbonate or bicarbonate are typically derived from dissolved carbon dioxide and not from dissolved oxygen, thus explaining why the amount of carbonate/bicarbonate ions are independent of the oxygen concentration in the flue gas. According to SEM-EDS, the amount of Fe on the surface of the tested specimen decreases as the oxygen concentration in simulated flue gas stream increases. On the other hand, the amount of O increases, whereas there is no change in the amount of S. This is probably due to the small amount of sulfur in the system relative to those of Fe and O. The amount of C increases slightly from its original value. Therefore, the products that are formed based on O and C on the tested surface are more measurable than those formed from S. These products include Fe(OH)₂, Fe(OH)₃, and FeCO₃. We have attempted to use the XRD technique to determine and verify the corrosion product formed on the specimen surface but could not get any meaningful result from this technique. It is possible that the corrosion products are either not in a crystalline form or are present in very minute amounts. As such, the use of the XRD technique appears not to be appropriate for this system.

3.1.2 Sulfur Dioxide Concentration

The results presented show that a higher sulfur dioxide concentration in the simulated flue gas stream induces more corrosiveness due to the increase in the solubility of SO₂, and generally, the formation of hydrogen ion (H⁺) or hydronium ion (H₃O⁺) [7-9]. Then, the oxidation-reduction of iron and hydronium ion occurs as in reaction 3.



SO₂ may react with water and oxygen and, then cause the corrosion of the carbon steel directly as shown in reactions 4-6 [10].



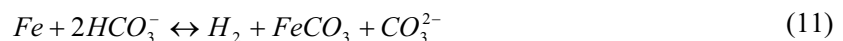
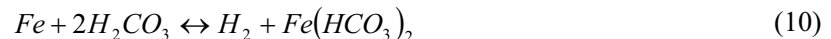
There is no significant difference in the amount of carbonate/bicarbonate in the systems by varying the SO₂ concentration. On the other hand, it was only for the high-concentration (204 ppm) SO₂ system that about 20 ppm of sulfate/bisulfite/sulfite anions were observed using the CE technique. From SEM-EDS we found that O and C slightly increase from the original amounts. S and O increase with increasing SO₂ concentration because of the formation of products that are composed of O, S, and C on the tested surface. These products include Fe(OH)₂, Fe(OH)₃, 2Fe₂O₃·H₂O, FeCO₃, and FeSO₄.

3.1.3 CO₂ Loading

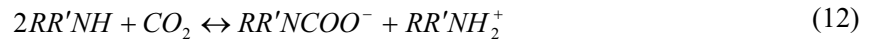
The corrosion rate increases dramatically with increasing CO₂ loading. The effect of CO₂ loading on corrosion is due to an increase in the concentration of carbonic acid (H₂CO₃) and bicarbonate (HCO₃⁻) that can induce the corrosion of iron. The formation of carbonic acid and bicarbonate are explained on the basis of reactions 7-9 [11].



The reduction-oxidation of iron with carbonic acid and bicarbonate ion are given in reactions 10 and 11.



It is also found that the amounts of bicarbonate and hydronium ions generally increase, as shown by reactions 12-14 [12].



It is seen from CE that carbonate and bicarbonate anions increase with increasing CO₂ loading. This is attributed to the increase in the amount of dissolved CO₂ in the system. The amounts of carbonate/bicarbonate anions are dominant in this system causing significant difference in corrosion rates of these systems. The result from SEM-EDS shows that the amount of Fe on the surface of the tested specimen decreased as the CO₂ loading increased, while O and S do not change much. C increased with increasing CO₂ loading because of increasing amounts of

dissolved CO₂ in the solution. Corrosion products are composed of O, S, and C on the tested surface. These products include Fe(OH)₂, Fe(OH)₃, 2Fe₂O₃·H₂O, FeCO₃, and FeSO₄.

3.1.4 MEA Concentration

The corrosion rate of the system increases sharply with MEA concentration. According to reactions 7-14, the higher the MEA concentration, the higher the total amount of CO₂ absorbed into the amine solution, resulting in higher amounts of reducible ions, HCO₃⁻ and H₃O⁺. These ions enhance the reduction rate, which induces a more rapid corrosion process. The result from CE shows an increase in the amount of carbonate/bicarbonate anions with higher MEA concentrations. This could be explained on the basis of an increase in the amount of absorbed CO₂ with increasing MEA concentration. The increase in carbonate/bicarbonate anion concentration is responsible for the increased corrosiveness of these systems. According to SEM-EDS, the amount of Fe on the surface of the tested specimen decreases as the MEA concentration increases. In contrast, C and S increase with increasing MEA concentration. On the other hand, there was no change in the amount of O with MEA concentration. The products responsible for the elemental distribution described include Fe(OH)₂, Fe(OH)₃, 2Fe₂O₃·H₂O, FeCO₃, and FeSO₄.

3.1.5 Operating Temperature

A higher temperature increases the corrosion rate of the system. The reason for the increase in corrosiveness with operating temperature can be explained on the basis of reaction kinetics that temperature generally accelerates the rate of any reaction [13]. All reactions mentioned in the previous section can go faster. The dissolved oxygen, H⁺ or H₃O⁺, H₂CO₃, and HCO₃⁻ enhance the reduction rate, and then, more metal is dissolved into the solution, thus leading to a higher corrosion rate. Also, not a significant amount of carbonate/bicarbonate anions are observed with increasing operating system temperature obtained by CE. The amounts of different elements on the tested specimen surface are obtained by the EDS technique. The amount of Fe on the surface of the tested specimen decreases as the temperature increases because of higher rate of corrosion. O, C, and S increase with increasing operating temperature which results from the products of corrosion that cover the specimen surface, including Fe(OH)₂, Fe(OH)₃, 2Fe₂O₃·H₂O, FeCO₃, and FeSO₄.

3.2 Corrosion Rate Correlation

An empirical power law type model (eq 15) for the liquid phase has been used to correlate corrosion rate with all the parameters in the MEA-H₂O-CO₂-O₂-SO₂ system.

$$CR = Ae^{(-H_a)/T} [SO_2]^{a_2} [O_2]^{a_3} [CO_2]^{a_4} [MEA]^{a_5} \quad (15)$$

where CR is the corrosion rate (mpy), A is the pre-exponential constant, H_a represents the temperature sensitivity of the electrochemical reaction (K⁻¹), T is the operating temperature (K), [SO₂], [O₂], [CO₂], and [MEA] denote the concentrations of SO₂, O₂, CO₂, and MEA (kmol/m³) in the solution phase, respectively, and a₂, a₃, a₄, and a₅ are the partial reaction orders with respect to SO₂, O₂, CO₂, and MEA, respectively. It should be noted that in the gas phase H_a is equivalent to E_a/R. The SO₂ concentration in the liquid phase was calculated from SO₂ concentration in the gas phase based on its solubility in water at various temperatures. The O₂ concentrations in the gas phase were used to calculate the dissolved oxygen in the liquid phase at a given pressure and temperature as shown in eq 16 [14].

$$[O] = -2.545 + 0.807 \times 10^{-2} T - 84.14 p + 2.096 \times 10^{-4} p T^2 + 2.322 \times 10^4 p/T + 1.027 p^2 - 3.911 \times 10^2 p^2/T \quad (16)$$

where $[O_2]$ is concentration of oxygen in millimoles per liter, T is temperature in Kelvin, and p is pressure in megapascals.

By using a nonlinear regression program (NLREG version 6.3), it was possible to determine all the constants in eq 15. The final corrosion rate correlation was thus obtained as eq 17.

$$CR = 1.77 \times 10^9 \left\{ \exp \left(-\frac{5,955}{T} \right) \right\} \times \{ [SO_2]^{0.0011} [O_2]^{0.0006} [CO_2]^{0.9} [MEA]^{0.0001} \} \quad (17)$$

The regression results show good regression statistics, with a coefficient of correlation (R^2) of 0.97. Also, a comparison of the experimental results with the corrosion rate model in terms of accuracy of the percentage average absolute deviation (%AAD) was 15.5%. Thus, this coefficient shows that the corrosion rate model adequately fits the corrosion rate data in the studied system.

3.3 Corrosion inhibitor

3.3.1 Inhibitor A

It was observed that the corrosion rate decreased from 211-61 mpy as the inhibitor A concentration was increased from 0 to 1000 ppm. Upon adding inhibitor A above 1000 ppm up to 5000 ppm, there was no significant change of corrosion rate and it still gave an average corrosion rate of 61 mpy. The inhibition efficiencies of A calculated by comparing its corrosion rate with the uninhibited system were in the range of 63-71%. The optimum concentration of inhibitor A was 1000 ppm and the inhibition efficiency was 71%.

3.3.2 Inhibitor B

Inhibitor B used was varied at concentrations of 0, 5, 10, and 25 ppm. Due to the limitation in the solubility of inhibitor B, higher concentrations of inhibitor B could not be carried out. The corrosion rate decreases to 211, 74, 65, and 51 mpy as the inhibitor B concentration increased from 0 to 5, 10, and 25 ppm, respectively. Comparing the corrosion rates of the systems with and without the inhibitor B, the inhibition efficiencies of inhibitor B were found to be 65, 69 and 76% for the respective inhibitor B concentrations. It can be concluded that the inhibitor B concentration of 25 ppm yielded the maximum inhibition efficiency of 76%.

3.3.3 Inhibitor C

The corrosion rate decreased tremendously from 211 to 5 mpy as the inhibitor C concentration was increased from 0 to 10,000 ppm. The inhibition efficiency of inhibitor C was calculated and found to be in the range of 84-98% for an increase in the inhibitor C concentration in the range of 10-10,000 ppm. At 1000 ppm of inhibitor C concentration, its efficiency was 95%. At higher inhibitor C concentrations of 5,000 and 10,000 ppm, the inhibition efficiency only slightly increased to 96% and 98%, respectively. Due to the cost of the chemical, 1,000 ppm was considered to be an optimum concentration.

3.3.4 Inhibitor D

The corrosion rate decreases from 211 to 60 mpy with increasing inhibitor D concentration from 0 to 1,000 ppm, and there is no significant change of corrosion rates above 1,000 ppm. At 5,000 and 10,000 ppm the corrosion rates decreased merely to 59 mpy. Thus, it could be stated that the optimum concentration of inhibitor D was at 1,000 ppm.

3.3.5 Inhibitor E

The corrosion rate decreases from 211 to 45 with increasing inhibitor E concentration from 0 to 5,000 ppm and there is no significant change of corrosion rate above 5,000 ppm. At 10,000 ppm, the corrosion rate of this system is still 45 mpy. Inhibition efficiencies obtained are varied from 44 to 79% upon addition of inhibitor E concentration from 10 to 1,000 ppm. A 5,000 ppm inhibitor E concentration was therefore considered as the optimum concentration that produced the highest inhibition efficiency of 79%.

3.3.6 Blended Inhibitor

The combination of inhibitors was chosen based on the initial proposal of inhibiting behavior. Inhibitors A, B, and C function by increasing the corrosion resistance of the metal surface, while inhibitor D functions by controlling the corrosive species in the solution. Synergistic effect of blended inhibitors was investigated using their optimum concentrations. Inhibitor D (1,000 ppm) mixed with each one of inhibitor A (1,000 ppm), B (25 ppm), and C (1,000 ppm).

The inhibitor A/D decreased the corrosion rate to 52 mpy corresponding to 75% inhibition efficiency, which was slightly more effective than the single inhibitor A or D alone. The blended inhibitor B/D yielded a corrosion rate of 45 mpy and an inhibition efficiency of 79%, thereby being more effective than the single inhibitors B or D. On the other hand, a blend of inhibitor C/D yielded the lowest corrosion rate of 7 mpy with 96% inhibition efficiency against the individual inhibitors.

4. Conclusions

We have shown for the first time that a higher concentration of SO₂ in a simulated flue gas stream will induce a higher corrosion rate because of the increase in hydrogen ion concentration generated by SO₂ and H₂O as well as SO₂, O₂, and H₂O. Also, iron may also react directly with SO₂ and O₂ to cause corrosion of carbon steel. Furthermore, analysis done for the first time shows that corrosion products generated from the effect of SO₂ include FeSO₄ and 2Fe₂O₃·H₂O.

An increase in oxygen concentration in simulated flue gas stream causes a higher corrosion rate due to increasing solubility of oxygen giving rise to a higher amount of dissolved oxygen in the liquid phase.

An increase in CO₂ loading and an increase in MEA concentration at constant CO₂ loading, which generally leads to an increase in the total amount of CO₂ absorbed into the amine solution, induces a higher corrosion rate since there is a resultant increase in hydrogen ion or hydronium ion, carbonic acid and bicarbonate ions generated by CO₂ and H₂O as well as the hydrolysis of carbamate and dissociation of protonated amine.

The corrosion rate increase with increasing temperature can be explained on the basis of reaction kinetics that temperature generally accelerates the rate of any reaction.

The use of Tafel plot and potentiodynamic techniques to study the effects of various variables on corrosion rate shows that these techniques provide very similar trends of information. The corrosion rates obtained from Tafel plot and potentiodynamic techniques are almost identical.

The corrosion products obtained experimentally based on CE and SEM/EDS techniques for the MEA-H₂O-CO₂-O₂-SO₂ system include Fe(OH)₂, Fe(OH)₃, 2Fe₂O₃·H₂O, FeCO₃, and FeSO₄.

A power-law model shows that corrosion rate of carbon steel increases with an increase in O₂ and SO₂ concentrations in simulated flue gas stream, as well as MEA concentration, CO₂ loading, and operating temperature. The CO₂ loading had the strongest impact on the corrosion rate, while SO₂ and O₂ show only slight effects on the corrosion rate.

Inhibitor A, B, C, D and E at the optimum concentrations of 1,000, 25, 1,000, 1,000 and 5,000 ppm were respectively found to be the most effective in minimizing the corrosion of carbon steel in MEA-H₂O-CO₂-O₂-SO₂ system, and produced inhibition efficiencies of 71, 76, 95, 72, and 79%, respectively.

Blends of A/D, B/D, and C/D using individual optimum concentration were found to be slightly better in terms of their inhibitive effect than their individual compounds.

5. Acknowledgement

The authors acknowledge the financial support from the Thailand Research Fund (TRF) through the Royal Golden Jubilee Ph.D. Program (Grant PHD/0204/2547) and from the Natural Science and Engineering Research Council of Canada (NSERC).

6. References

- [1] Veawab, A., Tontiwachwuthikul, P., Chakma, A. Corrosion Behavior of Carbon Steel in the CO₂ Absorption Process Using Aqueous Amine Solutions. *Industrial & Engineering Chemistry Research*. 1999; 38: 3917.
- [2] Soosaiprakasam, I. R., Veawab, A. Performance of copper carbonate as corrosion inhibitor in amine treating plants. 44th Annual Conference of Metallurgists of CIM held in conjunction with 35th Annual Hydrometallurgy Meeting, Calgary, Canada, August 21-24, 2005; NACE: Calgary, Canada, 2005.
- [3] Horeitz, W. Association of Official Analytical Chemists (AOAC) Methods, 12th ed.; George Banta: Wisconsin, U.S.A., 1975.
- [4] Kladkaew, N.; Idem, R.; Tontiwachwuthikul, P.; Saiwan, C., Corrosion Behavior of Carbon Steel in MEA-H₂O-CO₂-O₂-SO₂ system: *Industrial & Engineering Chemistry Research*. 2009, 48 (19), 8913.
- [5] Kladkaew, N.; Idem, R.; Tontiwachwuthikul, P.; Saiwan, C., Corrosion Behavior of Carbon Steel in MEA-H₂O-CO₂-O₂-SO₂ system: Products, Reaction Pathways and Kinetics. *Industrial & Engineering Chemistry Research*, 48 (23), 10169.
- [6] Fontana, M. G. *Corrosion Engineering*; 3rd ed.; McGraw-Hill, Inc.: New York, 1986.
- [7] Beutler, D.; Renon, H. Representation of NH₃-H₂S-H₂O, NH₃-CO₂-H₂O, and NH₃-SO₂-H₂O Vapor-Liquid Equilibria. *Industrial & Engineering Chemistry Process Design and Development*. 1978, 17, 220.
- [8] Castano, J. G., Arroyave, C., Morcillo, M. Characterization of atmospheric corrosion products of zinc exposed to SO₂ and NO₂ using XPS and GIXD. *Journal of Materials Science*. 2007, 42, 9654
- [9] Streeter, I., Wain, A. J., Davis, J., Compton, R. G. Cathodic Reduction of Bisulfite and Sulfur Dioxide in Aqueous Solutions on Copper Electrodes: An Electrochemical ESR Study. *Journal of Physical Chemistry B*. 2005, 109, 18500.
- [10] Sastri, V. S. *Corrosion Inhibitors*; John Wiley & Sons Ltd: Chichester, England, 2001.
- [11] Heuer, J. K., Stubbins, J. F. An XPS characterization of FeCO₃ films from CO₂ corrosion. *Corrosion Science*. 1999, 41, 1231.
- [12] Austgen, D. M., Rochelle, G. T., Peng, X., Chen, C. C. Model of Vapor-Liquid Equilibria for Aqueous Acid Gas-Alkanolamine Systems Using the Electrolyte-NRTL Equation. *Industrial & Engineering Chemistry Research*. 1989, 28, 1060.
- [13] Levenspiel, O. *Chemical Reaction Engineering*, 3rd ed.; John Wiley & sons: New York, 1999.
- [14] Rooney, P. C., Daniels, D. D. Oxygen solubility in various alkanolamine/water mixtures. *Petroleum Technology Quarterly*. 1998, 3, 97.